Quantum sampling AC standard for electrical power metrology based on programmable Josephson junction series array

Measurement 233 (2024) 114747

Contents lists available at ScienceDirect

Measurement

journal homepage: www.elsevier.com/locate/measurement

Quantum sampling AC standard for electrical power metrology based on programmable Josephson junction series array

Bruno Trinchera *, Paolo Durandetto, Danilo Serazio

INRIM-Istituto Nazionale di Ricerca Metrologica, Quantum Metrology and Nanotechnologies, Strade delle Cacce 91, 10135, Torino, Italy

ARTICLE INFO

Keywords:
Josephson voltage standard
Electric power measurement
High-precision digitizer
Voltage measurements
Comparison
Signal multiplexing

ABSTRACT

We report on the realization and preliminary validation of a quantum-based sampling power standard, based on a 1 V Programmable Josephson Voltage Standard (PJVS). The PJVS has been integrated into an existing sampling power standard along with a new synchronous multiplexer. Measurement scenarios for voltage and power measurements have been implemented and internally validated. Results of the measurement comparison against the Italian primary electrical power standard at 53 Hz agree well within the respective uncertainties, and did not exceed 15 μW/VA from 120 V to 240 V and 5 A and any power factor. Likewise, measurements of alternating voltage up to a few kilohertz show good agreement when compared against AC/DC voltage transfer method. The article illustrates the quantum power standard and its main constituents, measurement scenario, comparison results and discussion, along with a preliminary estimation of the uncertainty budget.

1. Introduction

The redefinition of the International System of Units (SI), which came into force in May 2019, marked a significant paradigm shift in the science of measurements, where dependencies from particular artifact-based standards and experimental realizations are now substituted with fundamental constants of nature. In particular, quantum-based standards play a crucial role in the revised SI for the practical realization of the units. For example, electrical power measurements could be linked to the fundamental constants of nature starting from DC power definition and Ohm's law, $U = I \cdot R$, as follow

$$P = U \cdot I \equiv I^2 \cdot R \equiv \frac{U^2}{R}, \tag{1}$$

The I, U and R quantities appearing in Eq. (1) were traced back in terms of fundamental constants by using

- the quantum current standard using the single-electron tunneling effect (SET):

$$I_{\mathrm{QS}} = e \times f_{SET}, \tag{2}$$

- the quantum voltage standard using the Josephson effect (JE):

$$U_{\mathrm{J}} = n\frac{h}{2e} f_J, \tag{3}$$

- the quantum resistance standard using the quantum Hall effect (QHE):

$$R_{\mathrm{H}} = \frac{h}{ie^2}, \tag{4}$$

where: e is the unit of electric charge, h the Planck constant, n the product between the Shapiro step order and the number of Josephson junctions, i is the plateau index, f_J is the irradiating microwave frequency and f_{SET} is the frequency controlling individually the tunneling of each electron. Both f_{SET} and f_J are traceable to the atomic frequency standard with negligible uncertainty (as low as 1×10^{-10}).

By combining the DC electrical quantum standards according to Eq. (1) and substituting I by I_{QS}, U by U_{J} and R by R_{H}, it is straightforward to get a set of equivalent mathematical expressions, reported in Table 1, which link electrical DC power to constants of nature, in particular to the product between Planck constant (h) and either one frequency squared or two distinct frequencies.

DC voltage and resistance reproductions by means of quantum standards were already exploited since 1990 to link the DC voltage and resistance measurements to the fundamental constants of nature. From a practical point of view, the combination of JVS and QHRS offers an interesting proof of concept and a straightforward route for establishing quantum traceability for DC power measurements in the framework of the revised SI. However, due to the current technological constrains, the pursuit of such a combination has not been addressed yet. Furthermore, accredited laboratories, in response to practical needs, require reliable power and energy measurements with lower uncertainties in alternating regime.

The use of quantum voltage standards, with particular emphasis on primary AC voltage metrology, began, more or less, over the

* Corresponding author.
E-mail address: b.trinchera@inrim.it (B. Trinchera).

https://doi.org/10.1016/j.measurement.2024.114747
Received 16 February 2024; Received in revised form 4 April 2024; Accepted 19 April 2024
Available online 26 April 2024

Table 1
Possible combination of electrical quantum effects linking electrical DC power unit to the constant of nature.

Quantum toolbox for electricity			Quantum standards combination
DC current (I_{QS})	DC voltage (U_J)	DC resistance (R_H)	DC power standard (P_{QS})
$e \cdot f_{SET}$	$(h/2e) \cdot f_J$	–	(JE & SET) $P_{QS} = I_{QS} \cdot U_J = (h/2) \cdot f_J f_{SET}$
$e \cdot f_{SET}$	–	h/e^2	(SET & QHE) $P_{QS} = I_{QS}^2 \cdot R_H = h \cdot f_{SET}^2$
–	$(h/2e) \cdot f_J$	h/e^2	(JE & QHE) $P_{QS} = U_J^2 / R_H = (h/4) \cdot f_J^2$

last decade. There has been growing interest in using Programmable Josephson Voltage Standards (PJVS) to characterize high-precision analog-to-digital converters (ADCs) and digital sampling multimeters (DSMs) [1–3], mainly used in power measurements, and to establish measuring methods [4–8] to link AC voltage measurements to the new SI, in order to improve the accuracy and speed up the measurement process compared to conventional AC/DC transfer methods.

Non-quantum power standards, based on synchronized high precision digitizing multimeters equipped with suitable voltage and current transducers, have been developed and routinely used by National Metrology Institutes (NMIs) [9–16] and industrial laboratories for practical power measurements with relative uncertainty far below 8 μW/VA (coverage factor, $k = 1$) at power-line frequency and any power factor.

A different traceability route using a single electrical quantum standard, i.e., the JVS, and the sampling strategy has been described in [17–21]. Inspired by these developments, the same strategy has been revised and further improved in the framework of the EMPIR project 19RPT01 - Quantum Power [22]. The main goal of the project was to design, develop and set up at least two quantum power standards (QPSs) by integrating existing PJVS into classical sampling power standards.

The practical realization of the quantum sampling electrical power standard has been accompanied by the development of a synchronous quantum power multiplexer (SQuP),[1] open source software [7], as well as measurement methods and algorithms suitable for providing real-time electrical power measurements, benefiting from permanent integration of the AC PJVS.

The paper is organized as follows: First, the main constituents of the quantum power standard are described. Second, the measurement scenarios implemented at the present stage of the development and experimental results carried out during the testing of QPS constituents are reported. Third, most recent achievements concerning the experimental results carried out with the QPS for the calibration of high-precision AC calibrators, characterization of ADCs and power meters at power line frequency are illustrated. Thereafter, a preliminary validation of the QPS measurement results against the AC electrical national standards for voltage and power is exhibited. Finally, the paper is discussed and concluded.

2. Quantum sampling power standard

The quantum power standard (QPS) has been designed and built using the modular concept, which allows for the swapping and reconfiguring of its main constituents according to the measurement scenarios.

Figs. 1 and 2 respectively report a simplified block diagram of the QPS setup and a photo of its implementation at INRiM.

[1] During the life time of the project, partners agree to call the synchronous power multiplexer "Synchronous Quantum Power Multiplexer (SQuP)", since it was purposely designed to be used with the PJVS. In the rest of the paper, the SQuP acronym will be used to identify the synchronous power multiplexer.

2.1. AC programmable Josephson voltage standard

The programmable Josephson voltage standard (PJVS) is a metrology-grade experimental setup, suitable to synthesize quantum-accurate direct-current (DC) voltages, whose quantum-accuracy is a direct consequence of the inverse AC Josephson effect. PJVSs are widely exploited as primary DC voltage standards [23,24], and have been further proven capable of generating stepwise-approximated sine waves. Moreover, when combined with appropriate sampling techniques, they enable the calibration of commercial AC equipment with a measurement uncertainty of parts in 10^7 up to a few kilohertz.

In the present development, the main purpose of the AC-PJVS is the real-time calibration of offset and gain of commercial high-precision ADCs or DSMs, using stepwise-approximated sine waves with frequencies up to few kHz.

A novel AC-PJVS setup has been designed and built up at INRiM in the framework of the project [22] using a commercial SNS (superconductor–normal–superconductor) array containing 8192 Josephson junctions (JJs). The JJs are divided into 14 binary segments in 64 parallel microwave stripline branches [25]. The number of JJs per stripline is 128 and the JJs between each two successive dc contacts are 1, 1, 2, 4, 8, 16, 32,..., 4096. Each segment of the array is current-biased independently using a software-controlled voltage source. For a SNS array containing 8192 JJs, the maximum output voltage at the RF frequency $f = 70.000000038324$ GHz, which is generated by a commercial RF synthesizer, when biased to the first Shapiro step is $U = 1.1857786427$ V. The weight of the low significant bit that correspond to the PJVS voltage resolution is $U_{LSB} = f \cdot (h/2e) = 144.738369$ μV.

The bias electronics used to switch on/off the single binary segments has been realized at INRiM starting from single commercial electronic boards. It has been further improved and updated with a new control software compared to the previous version described in [26]. Two commercial boards with up to 8 individually 16-bit digital-to-analog converters (DACs) are synchronized to a common update clock and trigger signals. The analog frequency of the stepwise-approximated sinewaves (f_a^{PJVS}) can be finely adjusted by tuning the frequency of the update clock, f_{Clk}, according to the expression, $f_a^{PJVS} = \frac{f_{Clk}}{N^{PJVS}}$, where N^{PJVS} represents the number of quantum-accurate DC voltage steps within a period.

The clock and trigger signals are provided by an additional high-speed DAC-based synthesizer, phase-locked to the 10 MHz distributed reference signal coming from the INRiM atomic clock. All DACs boards are fitted in a separate optically-isolated PXI chassis controlled by a dedicated PC. In general, up to 16 independent bias outputs are available, 13 of which are used to set the voltages across the array segments to $(-V_n, 0, +V_n)$, where V_n is the voltage of the nth channel of the bias electronics suitable to drive the nth array segment to the zero and first Shapiro steps.

The remaining outputs can be programmed for synthesis of suitable isofrequential sinusoidal and rectangular waveforms useful for synchronizing external equipment, such as AC generators, phantom power sources (PPSs) or multifunction calibrators to the PJVS bias source. Further details on the construction and characterization of the AC-PJVS are reported in [26].

2.2. Synchronous power multiplexer

The synchronous power multiplexer (SQuP) has been designed in the framework of the project [27] and some fully working implementations have been independently built by the project partners. In general, for the realization of a single SQuP unit, up to six independent slave boards are required in the configuration 2-to-1 (2-inputs to 1-output).

The outputs of two single 2-to-1 slave boards have been connected in parallel to form a single 4-to-1 slave board. The slave boards are

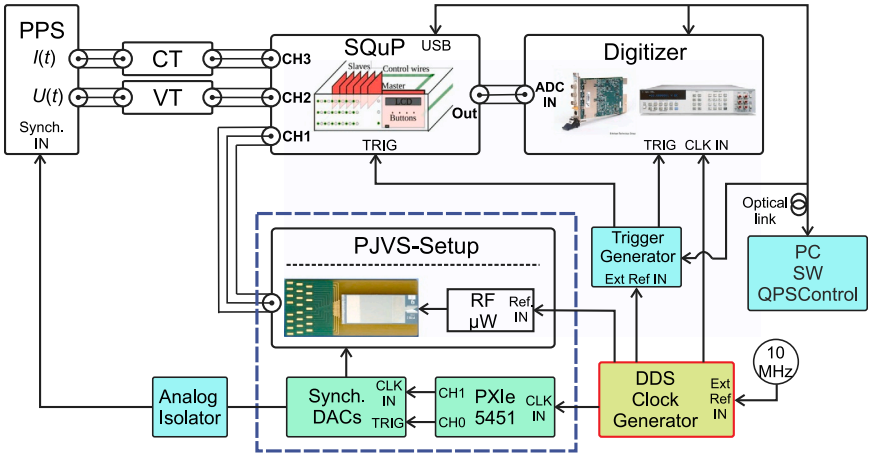

Fig. 1. Simplified schematic diagram of the QPS implemented at INRiM. PPS — Phantom power source (Fluke 6100A Calibrator); SQuP — Synchronous multiplexer; CT — Current transducer; VT — Voltage transducer; PJVS — Programmable Josephson voltage standard (Photograph of the PJVS reproduced with permission of Physikalisch-Technische Bundesanstalt (PTB)).

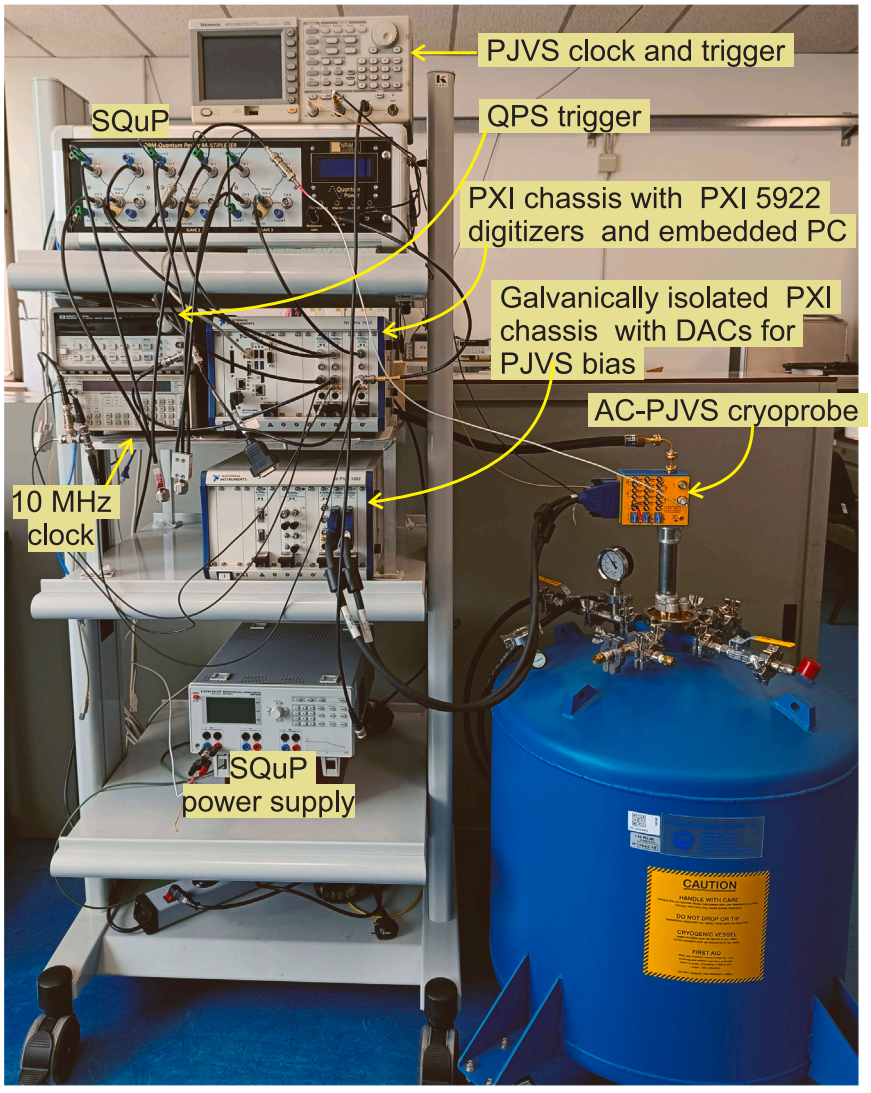

Fig. 2. Photo of the compact QPS experimental setup.

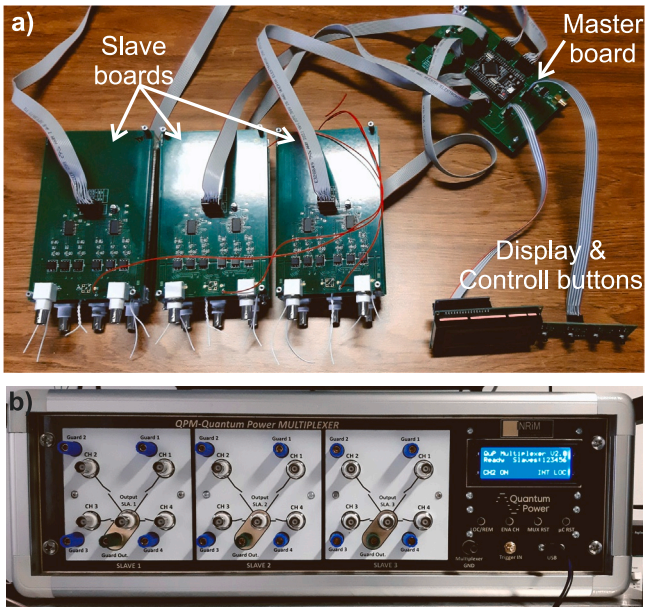

Fig. 3. (a) Set of the multiplexer boards. (b) photo of the SQuP developed at INRIM composed by three 4-to-1 slave boards.

equipped with PhotoMos solid-state relays (SSR)[2] which, compared to other solid-state relays, introduce lower errors and noise in the measurement system and present better DC characteristic and large dynamic range. In order to avoid short circuits between sources during the normal operation of the SQuP, the strategy break-before-make has been implemented, i.e., before setting the correct configuration, all switches are first opened and then, after a secure delay to prevent possible short circuits, closing only those interested.

The SQuP is remotely controlled using a master board based on an Arduino microcontroller connected to the PC by means of a USB interface. The switching sequence contains the on/off state of the single relays and is prepared via software in a matrix form. It is transferred from the PC to the master board. The on/off aperture time of the relays is controlled by a switching event, which can be generated internally using the internal SQuP clock or by applying an external synchronization signal to its trigger input. To avoid ground loops the trigger input has been optically isolated. Fig. 3 shows the full SQuP version built at INRiM.

2.3. Modular sampling standard

The sampling power standard identified for the integration of both PJVS and SQuP is part of the high frequency (HF) power and power quality modular macro-setup developed at INRiM in the framework of the project 15RPT04-TracePQM [28], which is based on wideband high-precision analog-to-digital converters (ADCs).

The low frequency (LF) part of the same modular macro-setup was developed for high-precision power measurement at power line frequencies and employs two synchronized digital sampling multimeters, e.g., DMM3458A, and voltage and current transducers. It has been validated in the framework of INRiM's participation during the EURAMET.EM-K5.2018 international comparison [29], where a relative measurement uncertainty ($k = 1$) within 8 µW/VA at any power factor and applied voltage and current 120 V to 240 V and 5 A, respectively, was demonstrated [15]. To achieve such a measurement uncertainty, an improved traceability chain has been implemented, where all the single constituents of the modular sampling power setup have been calibrated against DC and AC electrical national standards.

A further step towards improving uncertainty in power measurements consists of shortening the current traceability chain, switching from conventional and time consuming AC/DC transfer methods to quantum-based methods, by integrating AC-PJVS for real-time gain and linearity calibration of high-precision digitizers, as reported in the present work, and using AC-PJVS for the calibration of voltage and current transducers, under almost real operating conditions.

3. QPS measurement scenarios

One of the main features of the QPS concerns the introduction of a new measurement strategy based on the multiplexing of quantum and analog sine waves. Such a strategy enables simultaneous measurement and quantum-accurate calibration of low-voltage sine waves coming from voltage and current transducers. Moreover, it can be easily adapted for different purposes in electrical power measurement scenarios ranging from single-phase to three-phase power measurements using a single PJVS and a reduced number of ADCs. A proof of concept on the multiplexing strategies for quantum power measurement was described in [30].

The two main measurement scenarios implemented for testing and validating the QPS developed at INRiM are summarized below and a photograph of the overall experimental setup is shown in Fig. 4.

3.1. AC voltage measurements

As shown in Fig. 1, the QPS can be straightforwardly reconfigured via software for precise measurement of root-mean-square (rms) value of sinusoidal waves. In this sense, it allows the calibration of commercial calibrators and AC sources using a single SQuP slave board, connecting its inputs and output as follows:

- $CH1_{SQuP}$ input to the AC-PJVS output;
- $CH2_{SQuP}$ input to the output of the device under test (DUT), e.g. AC calibrator/source;
- SQuP output to the ADC input.

The proposed method differs from the differential sampling approach [5–8,20,21], because it does not require robust synchronization and frequency matching between the AC source and the AC-PJVS. However, in our experimental setup, we deal with the configuration in which the AC source is phase-locked to the AC-PJVS.

The synchronization has been performed by using a dedicated output channel of the AC-PJVS bias electronics, opportunely programmed to generate an isofrequential AC signal to the PJVS. Such a signal has been galvanically decoupled by using an isolation transformer and then applied to the phase lock-in input of the AC calibrator. The AC calibrator output signal is thereby frequency and phase synchronized to the Josephson staircase-approximated sine waves. The update clock of the AC-PJVS bias electronic and the sampling clock of the ADC are derived from the same 10 MHz reference signal, thereby coherent sampling can be exploited on the serialized waveform pattern at the SQuP output. The experimental results are reported in Section 4.3.

3.2. Single-phase power measurements at mains frequency

Fig. 1 reports the general schematic diagram for single-phase power measurements. The configuration uses a single SQuP slave board (2 channels for $U(t)$ and $I(t)$ signals and 1 channel for the $U_{PJVS}(t)$ reference signal) and a single ADC. This configuration is suitable for electrical power measurements using only 33% of the recorded stream,

[2] The PhotoMos-SSR are Vishay relays, where the output switch is a combination of a photodiode array with MOSFET switches. They can be configured for AC/DC or DC only operation. The on-resistance is about 0.25 Ω and turn on/off time is below 800 µs.

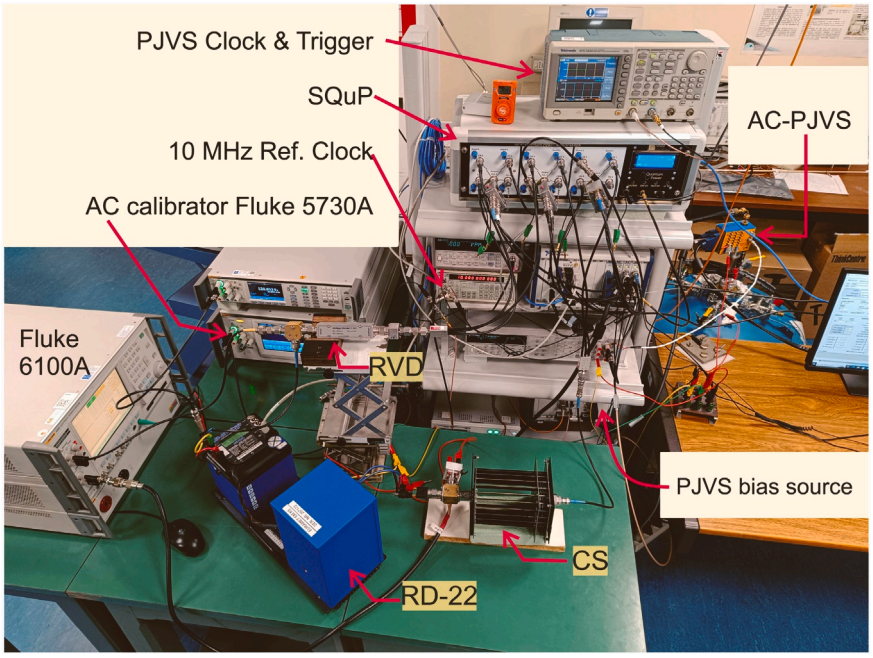

Fig. 4. Photo of the experimental setup implemented during the measurement campaign performed at INRiM (November 2023–January 2024) aimed for testing and validating the QPS used for calibration purposes of high performance multifunction calibrators (Fluke 5730A) and primary power transfer standards (Radian RD-22 Dytronic, accuracy class 0.005%).

Table 2
Connections matrix for arming the inputs and the outputs of the SQuP single slave boards with the signals coming from AC-PJVS, $U_{PJVS}(t)$, and voltage, $U(t)$, and current, $I(t)$, transducers. $\Delta(t_1) = \Delta(t_2) = \Delta(t_3)$ correspond to the switch-on time of each SQuP channel and are computed starting from the frequency of the analog signal and the number of periods. The output of each SQuP slave board is connected to a dedicated high-speed and resolution commercial digitizer.

SQuP slave boards	Input 1 $\Delta(t_1)$	Input 2 $\Delta(t_2)$	Input 3 $\Delta(t_3)$	Output
Board 1	CH1 $U_{\mathrm{PJVS}}(t)$	CH2 $U(t)$	CH3 $U(t)$	to ADC1
Board 2	CH2 $U(t)$	CH3 $U_{\mathrm{PJVS}}(t)$	CH1 $I(t)$	to ADC2
Board 3	CH3 $I(t)$	CH1 $I(t)$	CH2 $U_{\mathrm{PJVS}}(t)$	to ADC3

as described in [30]. The synchronization of external phantom power sources to the QPS could be done as in the previous scenario.

Extension to a second single-phase power measurement scenario using approximately 99% of voltage and current recorded waveforms has been implemented and extensively tested only recently using three SQuP slave boards, three ADCs boards and a single AC-PJVS. Table 2 shows the connections matrix of SQuP input and output signals.

A general overview of the connection scheme related to low-voltage part for single-phase power measurement scenario using all SQuP slave boards is depicted in Fig. 5. For ease of understanding, the voltage and current coaxial transducers are not shown.

Fig. 6 reports an example of the low-voltage side of the waveform stream at the output of each SQuP slave board digitized simultaneously. Each single stream of Fig. 6 is composed by an alternating sequence of two periods, $N_P = 2$, at frequency of $f_a = 53\,\mathrm{Hz}$, so the switch-on state for each SQuP channels is about $\Delta(t) = f_a \cdot N_P \approx 37.7\,\mathrm{ms}$, which corresponds to an external trigger frequency of about, $f_{\mathrm{Trig}}^{\mathrm{SQuP}} = 26.5\,\mathrm{Hz}$.

All timing parameters are set via software and almost all measurements have been carried out by fixing the number of periods to about $N_P = 20$, taking into account that approximately two periods are discarded at the beginning and at the end of each single frame of the stream. The measurement strategy implemented is based on

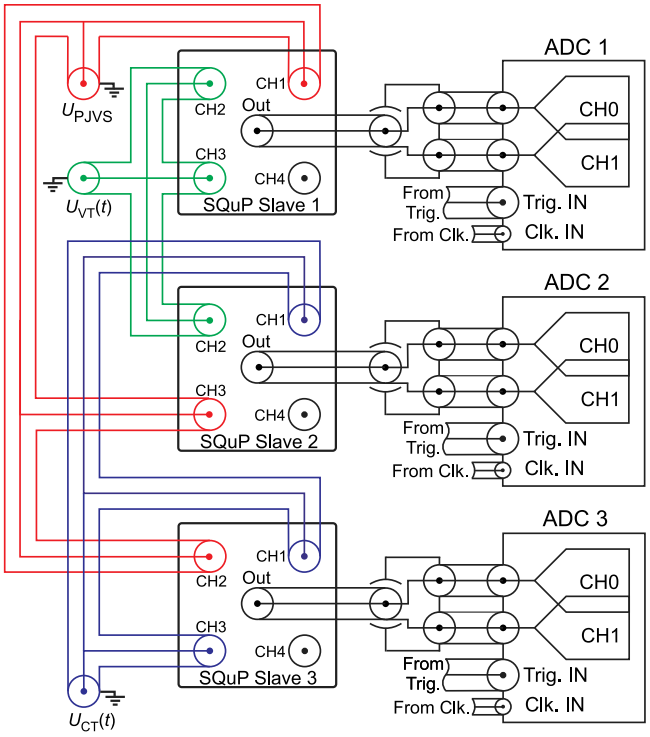

Fig. 5. Connection scheme for single-phase power measurements using three SQuP slave boards, three high speed ADCs ans one AC-PJVS. $U_{\mathrm{VT}}(t)$ represents the low voltage port of the voltage transducer (VT), which could be either a coaxial resistive voltage divider (RVD) or an inductive based voltage transducer, $U_{\mathrm{CT}}(t)$ represents the low voltage port of the current-to-voltage transducer, which could be either a current shunt or an inductive-based current transducer; U_{PJVS} represents the quantum based reference staircase sine-wave generated with the AC programmable Josephson voltage standard.

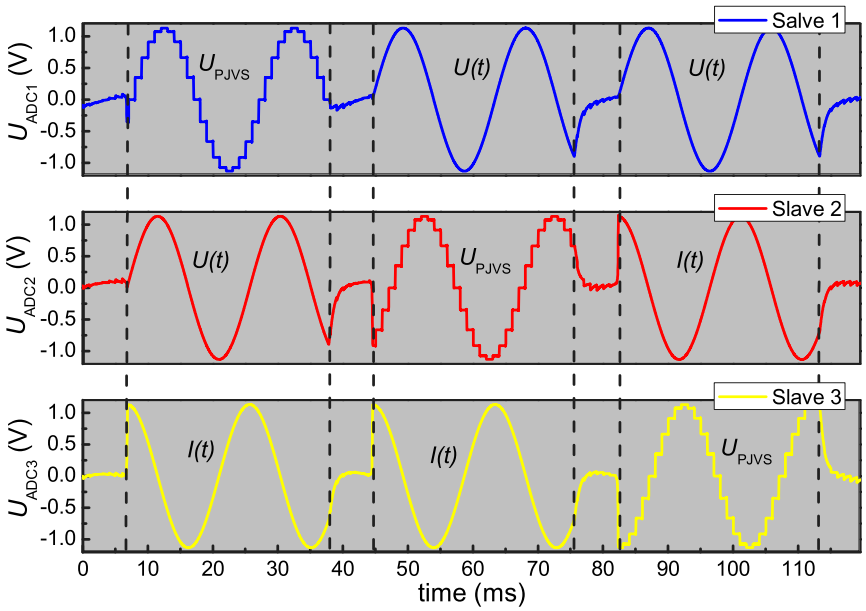

Fig. 6. Demonstration of the waveform stream at the output of the SQuP slaves. Each stream is composed of three frames containing approximately two periods of PJVS sine waves, U_{PJVS}, sinusoidal voltage signal, $U(t)$, and sinusoidal current signal, $I(t)$. All timing parameters are set and computed via software starting from the frequency of the analog signals, digitizer sampling frequency, and the number of periods within each frame.

data collection first and data processing immediately after. A single measurement stream could be composed of several alternating frames in series, so a large number of periods within each frame requires more time for data processing.

4. Experimental results and discussion

Experimental tests concerning the operation of the QPS as a whole, with particular emphasis to the characterization of its constituents and measurement scenarios described in Section 3, have been successfully performed. The measurement results are reported in the following subsections.

4.1. SQuP gain and phase characterization

Dedicated tests have been carried out to characterize the QPS constituents and in particular the SQuP slave boards. Since the SQuP performs the mixing of different analogue and quantum AC sine waves into a unique signal stream, its amplitude gain and phase delay errors related to each single channel become relevant and important to keep into consideration when high precision AC voltage measurements approaching the sub-ppm level are required.

The SQuP has been characterized in terms of amplitude gain and phase errors related to the single channels of the first slave board using two different measurement setups. The first setup is dedicated to the measurement of the amplitude gain error of SQuP single channels. It is based on the use of the AC-PJVS and a high precision DMM3458A. The measurement method consists in manually switching a DMM3458 between the input and output of each SQuP channel, while the channel state changes from OFF to ON.

By neglecting the short term stability due to the DMM gain variation between two consecutive measurements, the relative amplitude gain error of each SQuP channel is computed as follows:

$$\epsilon_{\mathrm{CH}}^{\mathrm{G}} = \frac{U_{\mathrm{CH}}^{\mathrm{ON}} - U_{\mathrm{CH}}^{\mathrm{OFF}}}{U_{\mathrm{PJVS}}} \cdot 1 \times 10^{6}, \tag{5}$$

where: $U_{\mathrm{CH}}^{\mathrm{ON}}$ is the voltage measured at the output of the SQuP slave boards when the state of channel under test is ON, U_{CH}^{OFF} is the voltage measured at input of the channel when its state is OFF, and U_{PJVS} is the theoretical rms value of the staircase Josephson sinusoidal waveform applied at the channel under test.

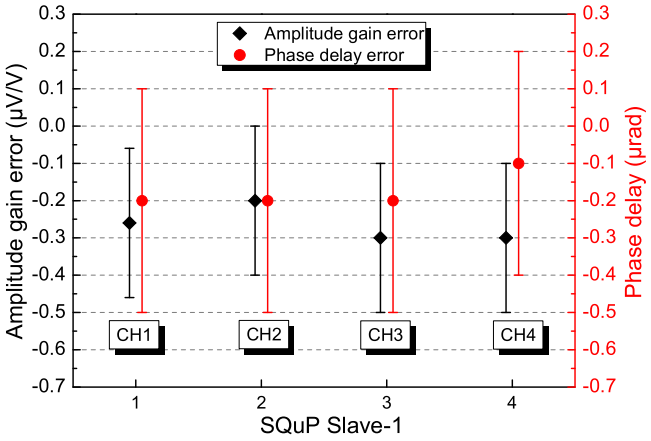

Fig. 7. SQuP gain and phase delay errors of the first SQuP slave. Measurements were carried out at 53 Hz and 800 mV.

For the determination of the phase delay error of the SQuP channels a second experimental setup based on a digital phase comparator has been used [31]. The AC test signal has been generated with a Fluke 5730A calibrator.

The characterization has been focused only the channels of the first SQuP slave board and the results are reported in Fig. 7. Error bars corresponds to Type A uncertainty, which is the most dominant component.

Further tests have been carried out on the other salve boards and the results found are similar. The test demonstrated that the relative gain and phase errors of the SQuP are less than 0.3 μV/V and 0.2 μrad and therefore their contribution to voltage or power measurements could be considered negligible at the mains frequency.

The cross-talk between the adjacent channels of the SQuP slave boards has been measured to be approximately −130 dB from 47 Hz to 65 Hz.

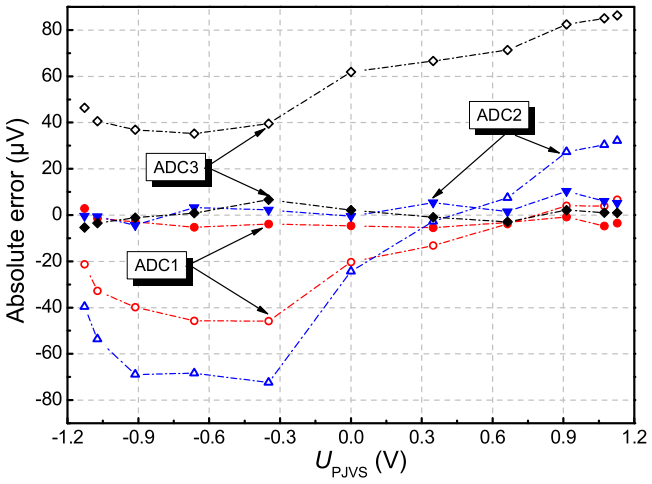

Fig. 8. Example on the effectiveness of the ADC calibration strategy implemented in the QPS setup. Empty symbols (red circles, blue triangles and black diamonds) represent the offset and gain error of each ADCs measured using stepwise-approximated Josephson sinusoidal waveform after removing the transients. Filled symbols represent the residual absolute offset and gain errors measured again using staircase-approximated Josephson sine waves after having corrected each ADC. The dash-dotted lines are guides to the eyes.

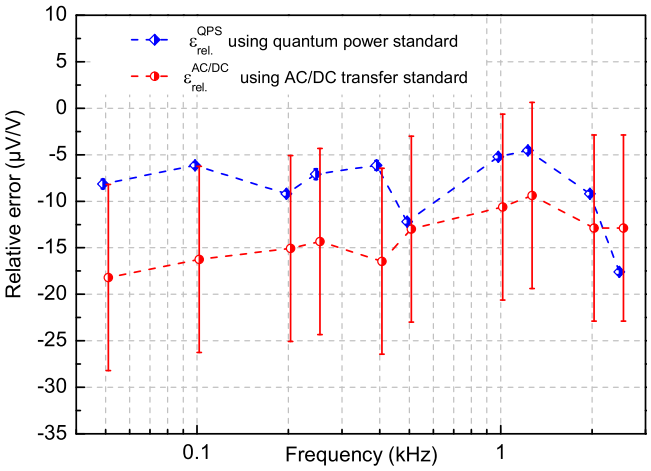

Fig. 9. Comparison results between QPS (blue-diamond) and conventional AC/DC transfer standard (red-circular) using an AC calibrator as transfer standard. Error bars indicate the expanded uncertainty ($k = 2$) as declared by INRiM's CMC (Calibration and Measurement Capabilities) associated to the calibration of AC calibrator using AC/DC transfer standard. Type A uncertainty relative to the measurements performed with the QPS remains below $0.3\,\mu V\,V^{-1}$ and the evaluation of further uncertainty components is under assessment. The dotted lines are guides to the eyes.

4.2. Gain and offset calibration of high-precision digitizers

Accurate gain and offset calibration of high precision digitizers is a relevant aspect for the measurement of the electrical quantities with the QPS. The effectiveness of the calibration strategy using the SQuP and the QPS has been proven and demonstrated experimentally and the results obtained are shown Fig. 8. The data shown in Fig. 8 refer to the absolute error, e_a, computed as the difference between the measured sampled voltage values and the theoretical values of each DC-step of PJVS sine wave. First, the PJVS sine wave is digitized by each ADC, then the calibration parameters such as gain and offset are extracted using a linear fit from the measured data. Secondly, the gain and offset parameters are used as correction factors, and the PJVS sine waves have been sampled again, and the absolute error recomputed. The overall ADC residual gain error remains below $0.2\,\mu V\,V^{-1}$ for all ADCs, demonstrating that the identified calibration strategy is suitable for reducing the contribution of uncertainty in power measurements due to digitizer calibration well below $1\,\mu V/V$. The measurements have been performed at 800 mV rms and 53 Hz.

4.3. Characterization of high-precision AC calibrator

A first demonstration concerning the measurement scenario employed by the QPS setup related to the calibration of a state-of-the-art AC calibrator[3] has been carried out in the frequency range from 50 Hz to 2.5 kHz and at 800 mV rms. The measurement results have been compared against a second measurement method based on the use of conventional AC/DC multirange electronic transfer standard. All measurements performed with the QPS have been carried out using a 20-step stepwise-approximated sine wave. The sampling frequency of the high resolution digitizer[4] was set to 5 MS/s and its vertical resolution is about 20 bits.

The relative error of the AC calibrator using QPS and AC/DC transfer methods has been computed as follow

$$\epsilon_{rel.}^{QPS,AC/DC} = \frac{U_M^{QPS,AC/DC} - U_N}{U_N} \cdot 1 \times 10^6, \tag{6}$$

where U_M^{QPS} and $U_M^{AC/DC}$ are the rms values of the AC calibrator measured with two different methods, i.e., with QPS and conventional AC/DC transfer standard, U_N is the nominal value.

Fig. 9 reports the relative error of the AC calibrator, $\epsilon_{rel.}$, measured with both methods. The measurements were completed within two-weeks with a short break between them. The maximum discrepancy between the methods is approximately $10\,\mu V/V$ at frequencies below 400 Hz, which may be due to the different measurement configurations of both methods. Further investigations focused on searching for possible systematic errors and ground loop effects are still in progress.

To summarize, this measurement campaign has been undertaken to demonstrate that the frequency extension of QPS, in its current implementation, paves the way for its use also for power measurements beyond the mains frequency and in the presence of distorted signals. The identified calibration strategy simplifies and speeds up the overall characterization process of high-precision digitizers, widely used for power and power quality measurements.

4.4. Comparison of QPS against INRiM's primary power standard

A first validation of the QPS has been carried out internally at INRiM. A measurement campaign aimed at the investigation of the whole QPS implementation in the configuration with three slave boards has been undertaken using state-of-the-art power transfer standard with true DC to AC transfer accuracy ±0.005%.[5] It has been provided by the National Metrology Institute of Germany, PTB, and circulated in a simple circular comparison scheme, among the participants who completed the QPS setup in their institutes (CMI, JV and INRiM) within the lifetime of the project. Each participant measured the calibration error of the traveling standard using their own QPS setups. The results of the comparison are still under evaluation.

[3] The calibrator was a high performance multifunction Fluke 5730A.

[4] The digitizer used in this work is NI PXI-5922 fitted in a high-bandwidth PXIe-1082 chassis equipped with a PXI embedded controller with Real-Time OS.

Brand names are used for identification purpose. Such identification does not imply recommendation nor does it imply that the equipment identified in this article is necessarily the best available for the purpose.

[5] The transfer power standard is a Radian model RD-22.

Here, we report the INRiM measurement results. The calibration error of the traveling standard, when measuring the active power, has been carried out at rated voltages 120 V to 240 V, current 5 A and power factors ($\lambda = 1,\ 0.5$ lead, 0.5 lag, 0 lead, 0 lag). The measurements have been performed using two different experimental setups:

(1) INRiM measurement system for primary power standard (MSPPS). The measurements have been performed in December 2023 and compared with a group of measurements carried out previously on the same traveling standard (RD-22) by INRiM [15], from January 2020 to February 2020, in the framework of the EURAMET.EM-K5.2018 key comparison.
(2) The quantum power standard (QPS) was handled in two different modes: (i) fully-automatic, using the open-source software developed during the project (QP_{SW}) [32], and (ii) semi-automatic, using an improved version of the INRiM's open tool traceable power quality analyzer (QTPQA) [33].

The main differences between the two QPS modes of operation consist of how the synchronous multiplexer is configured and used during the power measurements. In the fully-automatic mode, SQuP is configured and handled by the open tool software, QP_{SW}, in a true multiplexing mode, where the ADCs are always calibrated, as shown in Fig. 6. In the semi-automatic mode, SQuP is handled manually by its own QuMPX software [32]. The QPTQA software first performs ADC calibration using the AC-PJVS. Immediately afterward, it measures the signals coming from the respective voltage and current transducers without multiplexing them. In this mode ADC calibration is left to the needs of the end user.

The experience gained in managing both QPS modes of operation has had a significant impact on the entire measurement setup. On one hand, the semi-automatic mode of QPS operation presents some relevant features such as 100% digitizing of waveforms, continuous power monitoring, less noise and reduced hardware resources, i.e., only two SQuP slave boards and one or two ADC boards are required. Moreover, in the testing phase of the entire measurement setup, it allowed the identification of systematic measurement errors due to signal leakage, ground loops, interference between AC-PJVS and the ac sine waves, and the calibration strategy for voltage and current transducers. In particular, the conventional calibration strategy employed for voltage and current transducers has been reviewed and adapted to the QPS setup, but this topic deserves special treatment, which goes beyond the scope of this paper and is still being refined.

The relative difference between the active power measurements performed with the traveling standard (RD-22) and the INRiM power standard references is computed as

$$\Delta = \frac{P_{DUT} - P_S}{S}, \tag{7}$$

where P_{DUT} is the active power measurements of RD-22, P_S is the active power measurements of INRiM reference, $S = U \cdot I$ is the nominal apparent power.

The relative difference of the DUT was measured using a direct insertion connection similar to that described in [15] and shown in Fig. 4. The voltage input ports of both wattmeters are connected in parallel with the output of the phantom power calibrator and the current input ports are connected in series with the output current port of the same calibrator.

Fig. 10 reports the relative difference, Δ, of the measurements of the active power performed on the traveling standard at 120 V to 240 V, 5 A and different power factors. The differences in active power measurements between the different methods employed at INRIM to measure the error of the traveling standard are almost all within the best expanded measurement uncertainties ($k = 2$, coverage factor) of the primary power standard (MSPPS) and quantum power standard (QPS).

The measurement uncertainty reported in Fig. 10 has been computed as reported in [15]. One of the main achievement of the present

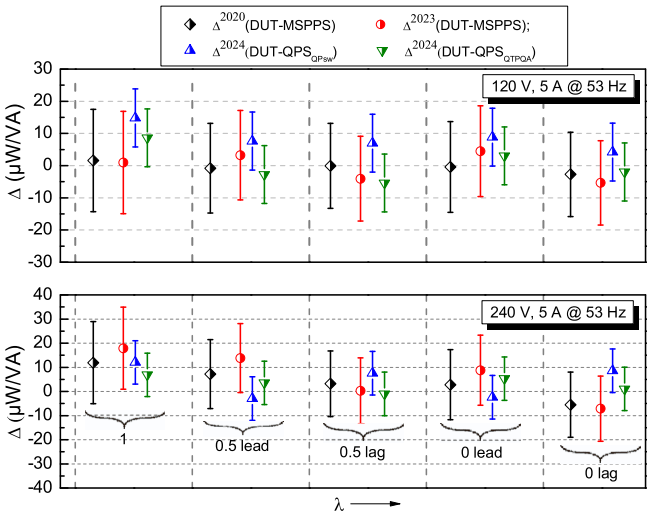

Fig. 10. Relative difference, Δ, of the active power measurements performed between the traveling standard (DUT) and INRiM's sampling power standards: MSPPS primary sampling standard; QPS_{SW} automatic and QPS_{QTPQA} semi-automatic quantum power standard implementations. Half-filled black diamonds and red circles, measurements performed in 2020 and December 2023 with the MSPS; half-filled blue and olive triangles, measurements performed in 2024 with the QPS in both modes. Uncertainty bars correspond to a 95% coverage factor.

work concerns the reduction of the uncertainty contribution in power measurements due to digitizers from 2 μV/V, as reported in [15], to better than 0.5 μV/V, using the PJVS setup.

The uncertainty budget of the QPS is still under evaluation. A first rough evaluation shows that the uncertainty contribution in power measurements due to voltage, current and phase measurements, taking into account the insertion of voltage and current transducers, at rated voltage 240 V and rated current 5 A, respectively, can be summarized as follow:

- Relative uncertainty for AC voltage measurement, using coaxial resistive voltage divider with nominal ratio $R_{RVD} = 1 : 301$, $u(U) = 3.0\,\mu V/V$;
- Relative uncertainty for AC current measurement, using coaxial current shunt with nominal resistance $R_{CS} = 0.16\,\Omega$, $u(I) = 3.0\,\mu A/A$;
- Phase angle measurement uncertainty, $u(\varphi) = 2.2\,\mu rad$,
- Combined relative standard uncertainty for active power measurements, $u(P)$,

$$u(P) = \sqrt{u^2(U) + u^2(I) + u^2(\varphi)} = 4.8\,\mu W/VA, \tag{8}$$

The expanded uncertainty, U, for active power measurements at any power factor using the QPS, to a first approximation, is within $U = 2 \cdot u(P) \approx 10\,\mu W/VA$.

It should be noted that the dependence on the resistance of the cables used in the cryoprobe and the room temperature connections was not considered in the preliminary estimation of the uncertainty budged reported. A first rough estimate indicates that this resistance, considering also the resistance of the SQuP, is approximately 1.7 Ω,[6] which compared to the 1 MΩ digitizer input impedance leads to a further uncertainty contribution of few parts in 1×10^6. This uncertainty

[6] Two center conductors of low-resistance coaxial cables, model CC-SC-25, each measuring 70 cm in length, were installed in the cryoprobe and their resistance is approximately 0.4 Ω. Taking into consideration the remaining cables length at room temperature, approximately 1 m, and the switch-on resistance of the multiplexer, which is approximately 0.25 Ω, the overall resistance from PJVS output to the ADC input is about 1.7 Ω.

contribution could be mitigated by utilizing digital sampling multimeters or by implementing custom high impedance buffers. However, further margins of improvement seem realistic, provided that the calibration strategy of voltage and current transducers is improved to make them immune from the loading effect of the input impedance of the digitizers.

5. Conclusion

A novel quantum sampling modular setup suitable for practical electrical measurements based on an AC programmable Josephson voltage standard (AC-PJVS) and a synchronous multiplexer (SQuP) has been built and extensively characterized.

Dedicated tests suited for precise characterization of all SQuP channels show that amplitude gain error and phase delay introduced by the channels are below 0.3 μV/V and 0.2 μrad, whereas Type A relative uncertainty is within 0.3 μV/V and 0.3 μrad, respectively. So, as a first approximation, their contribution during voltage measurements can be neglected.

The calibration strategy employed for real-time characterization of high precision digitizers, according to the QPS operation principle, has been tested proving that the parameters of interests, such as offset and gain, can be calibrated with quantum accuracy and the overall residual error remains below 0.2 μV/V over the tested frequency range, i.e., from 40 Hz to 2.5 kHz. Overall, the uncertainty contribution on power measurements at mains frequency due to the digitizers, has been proven to be less than 0.5 μW/VA.

Two different measurement scenarios have been set up and tested, one for AC voltage measurements up to a few kHz and the other for power measurements at typical mains frequency. The measurements carried out with the QPS have been compared with measurements performed against the AC voltage maintained standard, using a voltage calibrator as AC transfer standard. The differences found agree well with respect to the declared uncertainties. For voltage measurements, differences were lower than 10 μV/V below 400 Hz and reduced by a factor of two up to 2.5 kHz. Likewise, the comparative power measurements at 53 Hz and at any power factor using the QPS and the INRiM MSPPS show discrepancies within 15 μW/VA, which are in good agreement within the expanded uncertainty declared for the MSPPS [15], which do not exceed 16 μW/VA.

In conclusion, the obtained results are in good agreement with the QPS design expectations and are sufficient for the intended purpose. Furthermore, new experiments will be undertaken to test the capability of the QPS for measuring power under sinusoidal condition up to few kHz and in presence of distorted waveforms.

6. Future prospects

The obtained results pave the way for the extension of the QPS in the field of power measurements at higher frequencies, calibration of power quality analyzers, and characterization of synchronized voltage measurements required by grid operators

Continuing in this direction, it is also worth to mention that in the framework of the national project PRIN 2022 PNRR P20228WW42 QuantAGRID-*Next quantum-based traceability and new accuracy description for synchronized multifrequency phasor measurements in modern distribution grids* - INRiM is conducting research activities aimed at extending the capabilities of the QPS setup for accurate measurement of synchronized multifrequency phasor measurements. This research activity will also be supported by the new incoming EMP project (2024–2027) WAC-*Wideband quantum AC traceability*, which aims to extend the quantum traceability of AC waveforms and harmonics up to 100 kHz using low frequency AC-PJVS and suitable high-frequency sampling techniques.

CRediT authorship contribution statement

Bruno Trinchera: Writing – review & editing, Writing – original draft, Visualization, Validation, Supervision, Software, Resources, Project administration, Methodology, Investigation, Funding acquisition, Formal analysis, Data curation, Conceptualization. **Paolo Durandetto:** Writing – review & editing, Resources, Investigation, Formal analysis, Data curation, Conceptualization. **Danilo Serazio:** Resources, Investigation, Formal analysis, Conceptualization.

Declaration of competing interest

The authors declare the following financial interests/personal relationships which may be considered as potential competing interests: Bruno Trinchera reports financial support was provided by EURAMET European Metrology Programme for Innovation and Research. If there are other authors, they declare that they have no known competing financial interests or personal relationships that could have appeared to influence the work reported in this paper.

Data availability

The authors are unable or have chosen not to specify which data has been used.

Acknowledgments

This project (19RPT01 QuantumPower) has received funding from the EMPIR programme co-financed by the Participating States and from the European Union's Horizon 2020 research and innovation. The authors would like to thank R. Behr (PTB) for kindly providing the traveling power standard (Radian RD-22), M. Šíra (CMI) for his contribution to the development of QP_{SW} software and processing algorithms, R. Iuzzolino and M. E. Bierzychudek (INTI) for their contribution in the design of SQuP schematic and PCB as well as its firmware.

References

[1] W. Kürten, E. Mohns, R. Behr, J. Williams, P. Patel, G. Ramm, H. Bachmair, Characterization of a high-resolution analog-to-digital converter with a Josephson AC voltage source, IEEE Trans. Instrum. Meas. 54 (2) (2005) 649–652, http://dx.doi.org/10.1109/TIM.2004.843064.

[2] F. Overney, A. Rüfenacht, J.-P. Braun, B. Jeanneret, P.S. Wright, Characterization of metrological grade analog-to-digital converters using a programmable Josephson voltage standard, IEEE Trans. Instrum. Meas. 60 (7) (2011) 2172–2177, http://dx.doi.org/10.1109/TIM.2011.2113950.

[3] D. Henderson, J.M. Williams, T. Yamada, Application of a Josephson quantum voltage source to the measurement of microsecond timescale settling time on the Agilent 3458A $8\frac{1}{2}$ digit voltmeter, Meas. Sci. Technol. 23 (12) (2012) 124006, http://dx.doi.org/10.1088/0957-0233/23/12/124006.

[4] H.E. van den Brom, E. Houtzager, S. Verhoeckx, Q.E.V.N. Martina, G. Rietveld, Influence of sampling voltmeter parameters on RMS measurements of Josephson stepwise-approximated sine waves, IEEE Trans. Instrum. Meas. 58 (10) (2009) 3806–3812, http://dx.doi.org/10.1109/TIM.2009.2019720.

[5] A. Rüfenacht, C.J. Burroughs, S.P. Benz, P.D. Dresselhaus, B.C. Waltrip, T.L. Nelson, Precision differential sampling measurements of low-frequency synthesized sine waves with an AC programmable Josephson voltage standard, IEEE Trans. Instrum. Meas. 58 (4) (2009) 809–815, http://dx.doi.org/10.1109/TIM.2008.2008087.

[6] J. Lee, R. Behr, L. Palafox, A. Katkov, M. Schubert, M. Starkloff, A.C. Böck, An ac quantum voltmeter based on a 10 V programmable Josephson array, Metrologia 50 (6) (2013) 612, http://dx.doi.org/10.1088/0026-1394/50/6/612.

[7] C.J. Burroughs, A. Rüfenacht, S.P. Benz, P.D. Dresselhaus, Method for ensuring accurate AC waveforms with programmable Josephson voltage standards, IEEE Trans. Instrum. Meas. 62 (6) (2013) 1627–1633, http://dx.doi.org/10.1109/TIM.2013.2250192.

[8] A. Rüfenacht, C.J. Burroughs, P.D. Dresselhaus, S.P. Benz, Differential sampling measurement of a 7 V RMS sine wave with a programmable Josephson voltage standard, IEEE Trans. Instrum. Meas. 62 (6) (2013) 1587–1593, http://dx.doi.org/10.1109/TIM.2013.2237993.

[9] F.J.J. Clarke, J.R. Stockton, Principles and theory of wattmeters operating on the basis of regularly spaced sample pairs, J. Phys. E: Sci. Instrum. 15 (6) (1982) 645–652.

[10] G.N. Stenbakken, A. Dolev, High-accuracy sampling wattmeter, IEEE Trans. Instrum. Meas. 41 (6) (1992) 974–978.
[11] U. Pogliano, Use of integrative analog-to-digital converters for high-precision measurement of electrical power, IEEE Trans. Instrum. Meas. 50 (5) (2001) 1315–1318.
[12] G. Ramm, H. Moser, A. Braun, A new scheme for generating and measuring active, reactive, and apparent power at power frequencies with uncertainties of 2.5×10^{-6}, IEEE Trans. Instrum. Meas. 48 (2) (1999) 422–426, http://dx.doi.org/10.1109/19.769616.
[13] W.G.K. Ihlenfeld, E. Mohns, K. Dauke, Classical nonquantum AC power measurements with uncertainties approaching 1 μW/VA, IEEE Trans. Instrum. Meas. 56 (2) (2007) 410–413, http://dx.doi.org/10.1109/TIM.2007.890620.
[14] E. Mohns, G. Ramm, W.G.K. Ihlenfeld, L. Palafox, H. Moser, The PTB primary standard for electrical AC power, MAPAN 24 (2009) 15–19, http://dx.doi.org/10.1007/s12647-009-0004-z.
[15] B. Trinchera, D. Serazio, A power frequency modular sampling standard for traceable power measurements: Comparison and perspectives, IEEE Trans. Instrum. Meas. 71 (2022) 1–8, http://dx.doi.org/10.1109/TIM.2021.3132346.
[16] C. Mester, Sampling primary power standard from DC up to 9 kHz using commercial off-the-shelf components, Energies 14 (8) (2021) http://dx.doi.org/10.3390/en14082203, URL: https://www.mdpi.com/1996-1073/14/8/2203.
[17] L. Palafox, G. Ramm, R. Behr, W.G. Kurten Ihlenfeld, H. Moser, Primary AC power standard based on programmable Josephson junction arrays, IEEE Trans. Instrum. Meas. 56 (2) (2007) 534–537, http://dx.doi.org/10.1109/TIM.2007.891092.
[18] B.V. Djokić, Low-frequency quantum-based AC power standard at NRC Canada, IEEE Trans. Instrum. Meas. 62 (6) (2013) 1699–1703, http://dx.doi.org/10.1109/TIM.2013.2240952.
[19] L. Palafox, R. Behr, W.G.K. Ihlenfeld, F. Muller, E. Mohns, M. Seckelmann, F. Ahlers, The Josephson-effect-based primary AC power standard at the PTB: Progress report, IEEE Trans. Instrum. Meas. 58 (4) (2009) 1049–1053, http://dx.doi.org/10.1109/TIM.2008.2008862.
[20] B.C. Waltrip, B. Gong, T.L. Nelson, Y. Wang, C.J. Burroughs, A. Rufenacht, S.P. Benz, P.D. Dresselhaus, AC power standard using a programmable Josephson voltage standard, IEEE Trans. Instrum. Meas. 58 (4) (2009) 1041–1048, http://dx.doi.org/10.1109/TIM.2008.2011097.
[21] B.C. Waltrip, T.L. Nelson, M. Berilla, N.E. Flowers-Jacobs, P.D. Dresselhaus, Comparison of AC power referenced to either PJVS or JAWS, IEEE Trans. Instrum. Meas. 70 (2021) 1–6, http://dx.doi.org/10.1109/TIM.2020.3039647.
[22] 19RPT01-QuantumPower, Quantum traceability for AC power standards, 2020-2023, https://quantumpower.cmi.cz/.
[23] S. Solve, M. Stock, BIPM direct on-site josephson voltage standard comparison: 20 years of results, Meas. Sci. Technol. 23 (2012) 1–10, http://dx.doi.org/10.1088/0957-0233/23/12/124001.
[24] P. Durandetto, B. Trinchera, D. Serazio, E. Enrico, A 10 V PJVS-based DC voltage realization at INRiM, in: Proc. Conf. on IMEKO TC-4, Pordenone, Italy, 2023, pp. 117–121.
[25] B. Trinchera, D. Serazio, P. Durandetto, L. Oberto, L. Fasolo, Development of a PJVS system for quantum-based sampled power measurements, Measurement 219 (2023) 113275, http://dx.doi.org/10.1016/j.measurement.2023.113275, URL: https://www.sciencedirect.com/science/article/pii/S0263224123008394.
[26] B. Trinchera, V. Lacquaniti, A. Sosso, M. Fretto, P. Durandetto, E. Monticone, On the synthesis of stepwise quantum waves using a SNIS programmable Josephson array in a cryocooler, IEEE Trans. Appl. Supercond. 27 (4) (2017) 1–5, http://dx.doi.org/10.1109/TASC.2016.2636569.
[27] M.E. Bierzychudek, R. Iuzzolino, H. Malmbekk, M. Šíra, B.O. Trinchera, An SSR-based multiplexer for power measurement, in: Proc. Conf. on Precision Electrom. Meas., Wellington, New Zealand, 2022, pp. 1–2.
[28] 15RPT04-TracePQM, Traceability Routes for Electrical Power Quality Measuremen, EMPIR project, 2016-2019, https://www.euramet.org/research-innovation/search-research-projects/details/project/traceability-routes-for-electrical-power-quality-measurements.
[29] KCBD, EURAMET.EM-K5.2018 - Key comparison of 50/60 Hz power, 2019-2020, https://www.bipm.org/kcdb/comparison?id=1620.
[30] M. Šíra, H. Malmbekk, B. Trinchera, R. Iuzzolino, M.E. Bierzychudek, Multiplexing schemes for quantum power systems, in: Proc. Conf. on Precision Electrom. Meas., Wellington, New Zealand, 2022, pp. 1–2.
[31] B. Trinchera, D. Serazio, U. Pogliano, Asynchronous phase comparator for characterization of devices for PMUs calibrator, IEEE Trans. Instrum. Meas. 66 (6) (2017) 1139–1145, http://dx.doi.org/10.1109/TIM.2017.2648598.
[32] M. Šíra, QPsw - Quantum Power software, 2022, https://github.com/KaeroDot/QPsw.
[33] B. Trinchera, S. Mašláň, TPQA-traceable power & power quality analyzer, 2019, URL: https://github.com/btrinchera/TPQA.